Journal of the European Ceramic Society 22 (2002) 79–85

www.elsevier.com/locate/jeurceramsoc

Formation mechanism and sintering behavior of $Ba_2Ti_9O_{20}$

Tsang-Tse Fang *, Jyh-Tzong Shiue, Sz-Chain Liou

Department of Materials Science and Engineering, National Cheng Kung University, Tainan, Taiwan, 701, ROC

Received 15 December 2000; received in revised form 22 February 2001; accepted 4 March 2001

Abstract

The reaction mechanism of a mixture of $BaTi_4O_9$ and TiO_2 was investigated. It was found that the development of $Ba_2Ti_9O_{20}$ was not via the direct reaction of $BaTi_4O_9$ and TiO_2 at the interface, but by nucleation from the matrix of $BaTi_4O_9$ inserted by the Ti species in the limited temperature range of 1200–1300°C. It is suggested that the formation of $Ba_2Ti_9O_{20}$ is via nucleation and growth. Moreover, it was observed that twinning existed in the remaining $BaTi_4O_9$ grains during the formation processes, which is due to the fact that the retained $BaTi_4O_9$ grains were stressed by the surrounding $Ba_2Ti_9O_{20}$ grains. Possible explanations for the difficulty in preparing $Ba_2Ti_9O_{20}$ are proposed. A sample with a high-density (about 99% theoretical density) and fine-grained uniform microstructure could be achieved and the dielectric properties are dielectric constant 39, Q 5863 at 7.3 GHz, and the temperature coefficient of resonance frequency 5 ppm/°C.

Keywords: $Ba_2Ti_9O_{20}$; Dielectric properties; Microstructure-final; Reaction sequence

1. Introduction

The recent advancement of the microwave wireless communication could be attributed to technologic improvement of the dielectric resonator. Efforts have been put on the miniaturization of the microwave circuitry. Dielectric resonators with large values of permittivity meet this function. A combination of high dielectric constant, high Q factor, and low temperature coefficient of resonant frequency[1–3] is required for a high-quality dielectric resonator. Jonker and Kwestroo[4] reported that single-phase $Ba_2Ti_9O_{20}$ could only be obtained by doping small amounts of SnO_2 or ZrO_2. However, it has been shown[5] that single-phase $Ba_2Ti_9O_{20}$ could be synthesized without doping near 1300°C but decomposed at temperatures above 1300°C. While a few reports[6,7] using wet chemical methods could synthesize $Ba_2Ti_9O_{20}$ at low temperatures (<1000°C), most papers[8–10] showed that it could only be obtained by calcining at high temperatures $\geqslant 1200$°C for a long time. The sluggish formation of $Ba_2Ti_9O_{20}$ has been attributed to the increase of distance between intermediate phases,[10–12] high surface and interface energies,[8] or the high potential energy barrier arising from the crystal structure.[13] Therefore, it is apparent that the formation mechanism and low formation rate of $Ba_2Ti_9O_{20}$ still needed to be clarified. Moreover, owing to the difficulty in synthesizing the high-quality single-phase $Ba_2Ti_9O_{20}$, its sintering behavior so far has been rarely studied.

In this investigation, the formation mechanism and sintering behavior of $Ba_2Ti_9O_{20}$ were intensively studied.

2. Experimental procedure

The starting materials used in this investigation were reagent-grade $BaCO_3$ (99.9%, 325 mesh, CERAC Inc., Milwaukee, USA) and TiO_2 (99.9%, 325 mesh, CERAC Inc., Milwaukee, USA). $BaTi_4O_9$ was prepared directly from $BaCO_3$ and TiO_2 in an appropriate ratio. $Ba_2Ti_9O_{20}$ was synthesized via two ways : $BaCO_3$ with TiO_2 and $BaTi_4O_9$ with TiO_2 in appropriate ratios. These powders were mixed for 24 h in a Nylon jar containing ZrO_2 balls and ethyl alcohol. The mixed powders were rapidly dried by microwave to reduce the segregation. Subsequently, the powders were ground lightly with a mortar and pestle and then pressed as a pellet. These pellets were calcined in air at different temperatures without holding but at 1200°C, different times were also performed. The formed single-phase $Ba_2Ti_9O_{20}$ powder

* Corresponding author. Tel.: +886-6-275-7575; fax: +886-6-234-6290.

E-mail address: ttfang@mail.ncku.edu.tw (T.-T. Fang).

0955-2219/01/$ - see front matter
PII: S0955-2219(01)00244-8

was used for sintering study. The sintering behavior was carried out in a dilatometer at different temperatures.

An X-ray diffractometer (Model D/MAX III.V XRD, Rigaku, Tokyo, Japan) was used for determining the phases and the reaction amount. The procedure for determining the reaction amount is described as follows. The powder compacts was sintered at 1200°C for different times and then quenched in air for evaluating the reaction amount. The internal standard method[14] was employed to determine the developing amount of $Ba_2Ti_9O_{20}$, in which the quenched samples were ground and SiO_2 (quartz) was used as an internal standard. The scanning rate was set to 1° per min over a range of 22–31°. These peaks, with the strongest intensity of diffraction were selected to measure the extent of $Ba_2Ti_9O_{20}$ and the collected counts of the peaks were fitted and integrated to extract the peak area. Transmission electron microscopy (TEM) (JEM-2010 (for Figs. 5 and 6) and JEM-3010 (for Fig. 8), Jeol, Japan) and high resolution transmission electron microscopy (HF-2000, Hitachi, Japan) were employed to identify the phases using selected area diffraction pattern (SADP) and examine the microstructures.

For dielectric measurement, the sintered pellets were cut perpendicular to the cylindrical axis to form parallel faces and their side walls were ground. The relative dielectric constant, Q value, and temperature coefficient of resonant frequency at microwave frequencies were investigated using the method proposed by Hakki and Coleman[15] and developed by Kobayashi and Tanaka.[16] A microwave network analyzer (Model 8510C, pulsed-RF network analyzer, Hewlett-Packard Co., Santa Clara, CA) was used to measure the microwave properties.

3. Results

Fig. 1 shows X-ray diffraction (XRD) patterns of the formation processes of $Ba_2Ti_9O_{20}$ by calcining the mixture of $BaCO_3$:TiO_2 = 1:4.5 at different temperatures without holding. It was observed that minute $BaTiO_3$ occurred first at 800°C and disappeared above 1000°C. $BaTi_4O_9$ appeared at 900°C and almost dominated at 1200°C. It should be noted that TiO_2 has completely disappeared at 1200°C but $Ba_2Ti_9O_{20}$ still was not observed. Fig. 2 shows XRD patterns of the mixture of $BaCO_3$:TiO_2 = 1:4.5 isothermally heated at 1200°C for different times. It was observed that $Ba_2Ti_9O_{20}$ appeared in 3 h but could not be completely formed with longer time. Fig. 3 shows the XRD patterns of the formation processes of $Ba_2Ti_9O_{20}$ by calcining the mixture of $BaTi_4O_9$:TiO_2 = 2:1 at different temperatures without holding. As observed, $BaTi_4O_9$ remained almost unchanged but TiO_2 disappeared at temperatures >1000°C. Fig. 4 shows the isothermal calcination of the mixture of $BaTi_4O_9$:TiO_2 = 2:1 at 1200°C for different times. It is

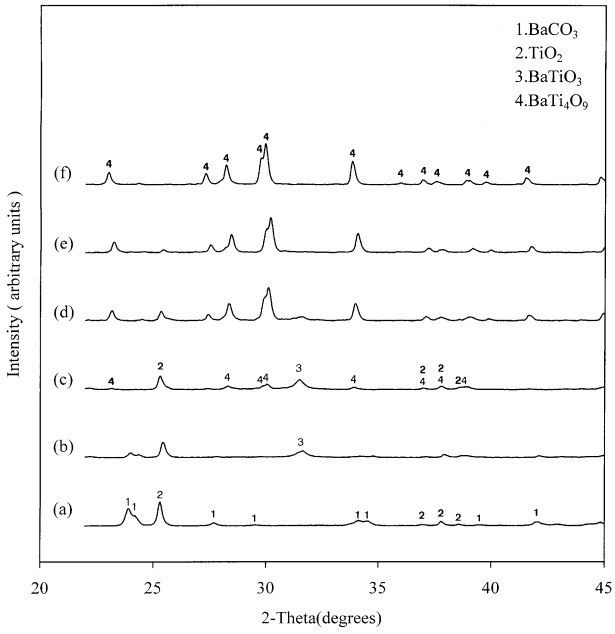

Fig. 1. X-ray diffraction patterns of the mixture of $BaCO_3$ and TiO_2 calcined at different temperatures without holding : (a) mixture, (b) 800°C, (c) 900°C, (d) 1000°C, (e) 1100°C and (f) 1200°C.

apparent that $Ba_2Ti_9O_{20}$ could more easily develop by calcining the mixture of $BaTi_4O_9$ and TiO_2 comparing with Fig. 2. Moreover, though $BaTi_4O_9$ has reduced to a minute amount in 3 h, it took more than 20 h to completely eliminate this retained $BaTi_4O_9$.

Fig. 5 shows the bright-field image (BFI) and selected area diffraction pattern (SADP) of TEM for the mixture of $BaTi_4O_9$:TiO_2 = 2:1 calcined at 1150°C without hold-

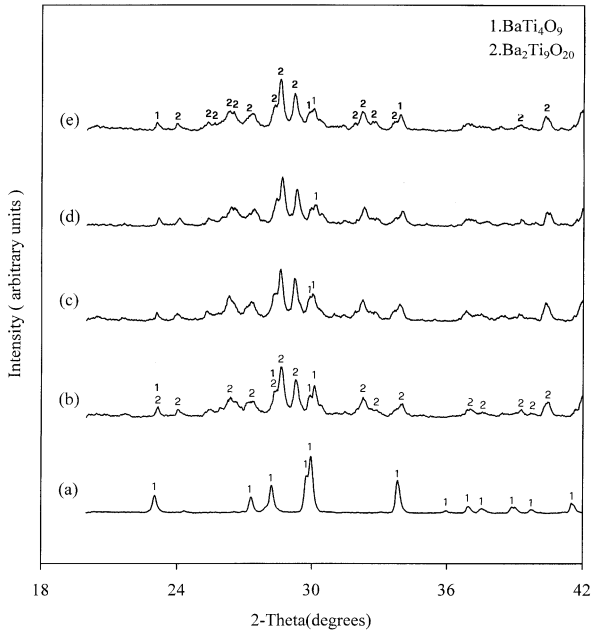

Fig. 2. X-ray diffraction patterns of the mixture of $BaCO_3$ and TiO_2 isothermally heated at 1200°C for different times : (a) 0 h, (b) 3 h, (c) 6 h, (d) 9 h and (e) 12 h.

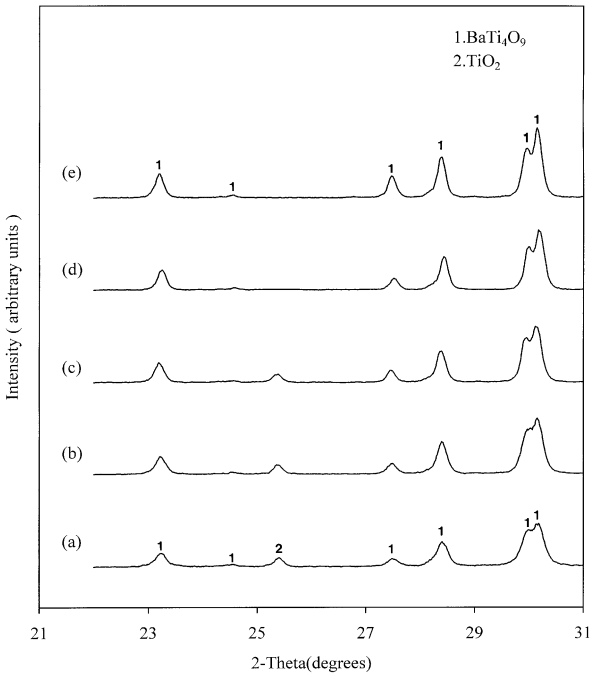

Fig. 3. X-ray diffraction patterns of the mixture of $BaTi_4O_9$ and TiO_2 calcined at different temperatures without holding : (a) 800°C, (b) 900°C, (c) 1000°C, (d) 1100°C and (e) 1200°C.

ing. It is interesting to show that based on the analysis of SADP, the calcined phase was identified as the structure of $BaTi_4O_9$. Moreover, there are not only some spots are not spherical but also many extra spots also appear in SADP, which implies that Ti species might diffuse in the $BaTi_4O_9$ without reaction and distort its lattice. Fig. 6 shows the BFI and SADP of the mixture of $BaTi_4O_9$: TiO_2 =2:1 calcined at 1200°C for 3 h. Based on the analysis of SADP, these nanometered grains (≈ 50 nm) observed at the local area of the sample were identified as the $Ba_2Ti_9O_{20}$. Among the solid state reaction models,[17] the Johnson–Mehl–Avrami (JMA) equation ($-\ln(1-x)=kt^n$)based on the model of the nucleation and growth,[18,19] was found to have the best fit, shown in Fig. 7. The value of n representing the slope was evaluated as 0.5, which suggests that the particle shape is lath-shaped,[17] supported by the microstructure shown in Fig. 8. Fig. 9 shows that most residual $BaTi_4O_9$ grains reveal twinning when $Ba_2Ti_9O_{20}$ was apparently developed, which indicates that the residual $BaTi_4O_9$ grains might be stressed by $Ba_2Ti_9O_{20}$ grains. Fig. 10 shows isothermal sintering behavior at different temperatures. The average activation energy about 1320 kJ/mol was evaluated in Fig. 11.

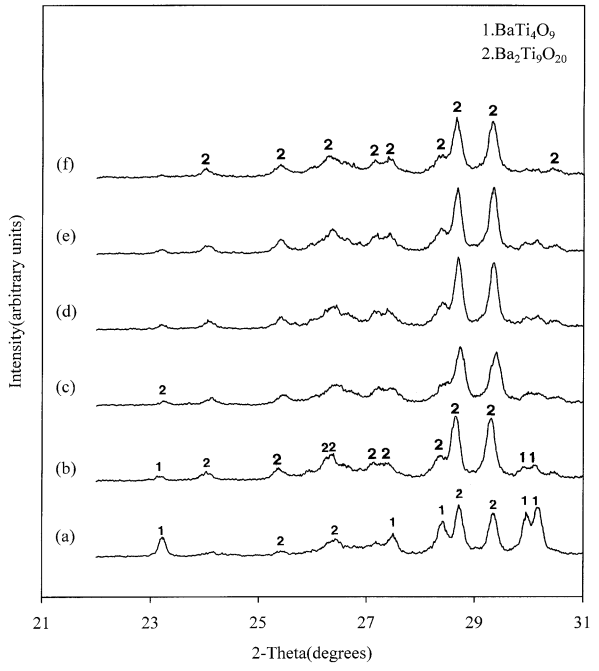

Fig. 4. X-ray diffraction patterns of the mixture of $BaTi_4O_9$ and TiO_2 isothermally heated at 1200°C for different times : (a) 1 h, (b) 3 h, (c) 9 h, (d) 15 h, (e) 20 h and (f) 30 h.

4. Discussion

Two intermediate phases, i.e., $BaTi_4O_9$[1,4,5,11,20] and $BaTi_5O_{11}$[6,8–10,20,21] were reported in forming $Ba_2Ti_9O_{20}$. However, it should be pointed out that $BaTi_5O_{11}$ was never observed in using the solid-state reaction.[1,4,5,11,22]

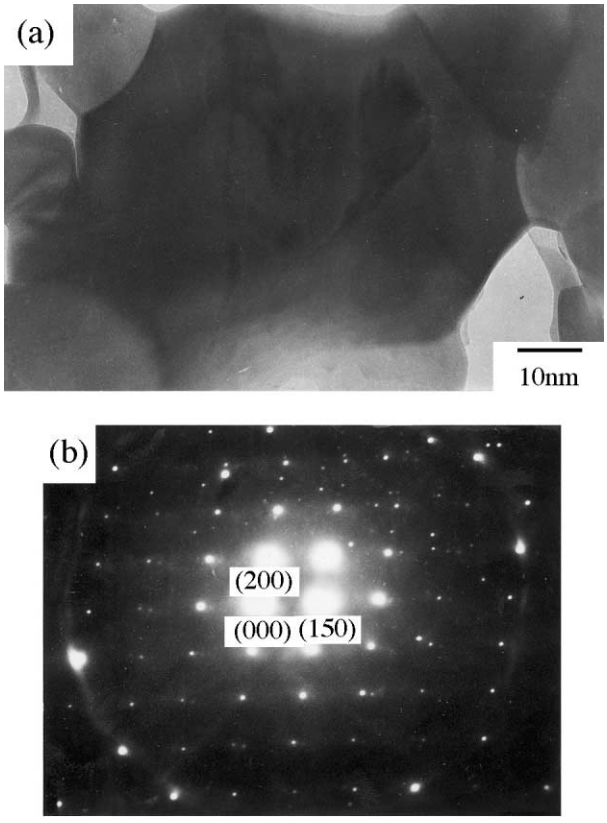

Fig. 5. (a) TEM bright-field image and (b) selected area diffraction pattern (zone axis: [0 0 $\overline{1}$0]) for the mixture of $BaTi_4O_9$ and TiO_2 calcined at 1150°C without holding.

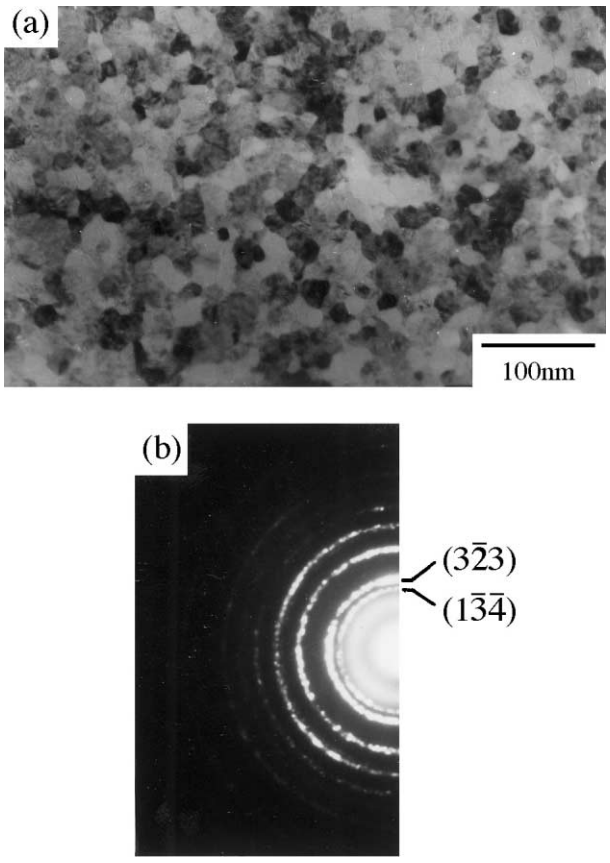

Fig. 6. The mixture of $BaTi_4O_9$ and TiO_2 calcined at 1200°C for 3 h showing the possible $Ba_2Ti_9O_{20}$ nuclei (a), identified by the selected area diffraction pattern (b).

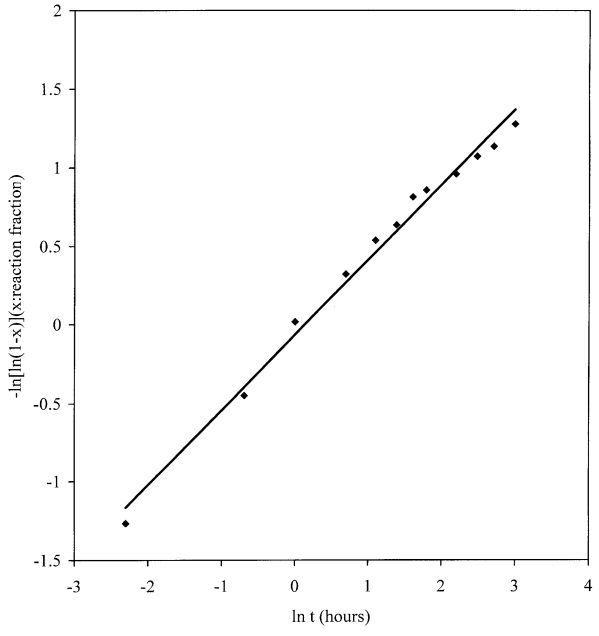

Fig. 7. Scaled reaction data fitted by the nucleation-growth model (Johnson–Mehl–Avrami equation).

This implies that mechanical mixing would be difficult in preparing a very high ratio of Ti/Ba, due to the fact that some precursor phase with a lower Ti/Ba ratio would form first and further reaction would have ions diffuse over a longer distance to form the desired phase. $Ba_2Ti_9O_{20}$ was also reported to have such a problem.[11] In comparing Figs. 2 and 4, it was shown that under the same preparation conditions, the use of a mixture of $BaTi_4O_9$ and TiO_2 has smaller amount of $BaTi_4O_9$ remaining than that of $BaCO_3$ and TiO_2 in forming $Ba_2Ti_9O_{20}$, which supports that the mixing might be a reason to explain the sluggish formation of $Ba_2Ti_9O_{20}$. However, the reason why the formation temperature was restricted in a very limited range of 1200–1300°C would need to be further discussed.

Wu and Wang[8] attributed the difficulty in preparing $Ba_2Ti_9O_{20}$ to the high interface energy of $Ba_2Ti_9O_{20}$, based on the so-called bumps occurring at the grain boundaries shown in their microstructure. However, the so-called bumps could usually be observed in the ceramic microstructure with the second phase existing at the grain boundaries.[23] Moreover, the bumps were not observed in this investigation. Thus, in our opinion, the

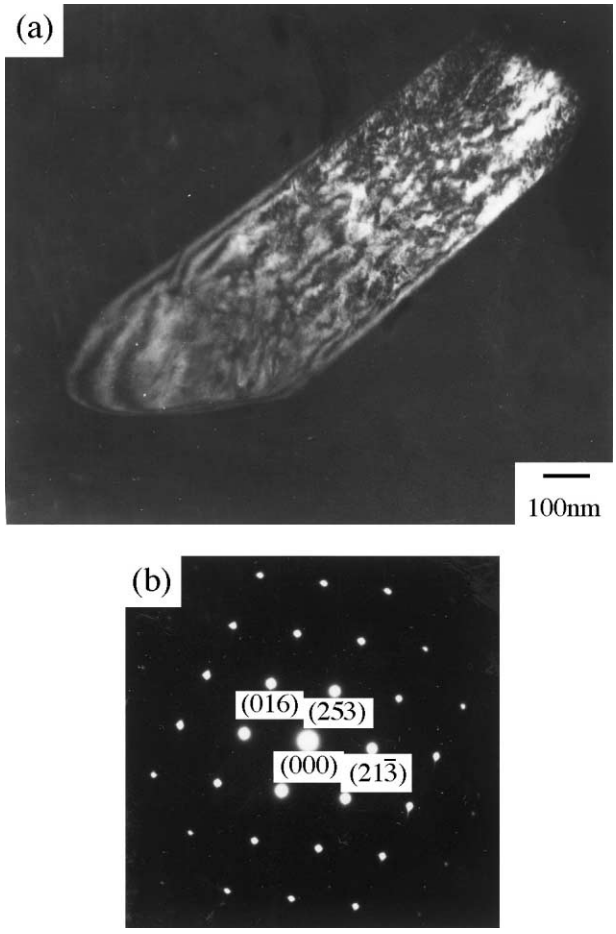

Fig. 8. The mixture of $BaTi_4O_9$ and TiO_2 calcined at 1200°C for 0.5 h showing the lath-shape particle (a), which was identified as $Ba_2Ti_9O_{20}$ by the selected area diffraction pattern (zone axis: [9 $\overline{12}$ 2]) (b).

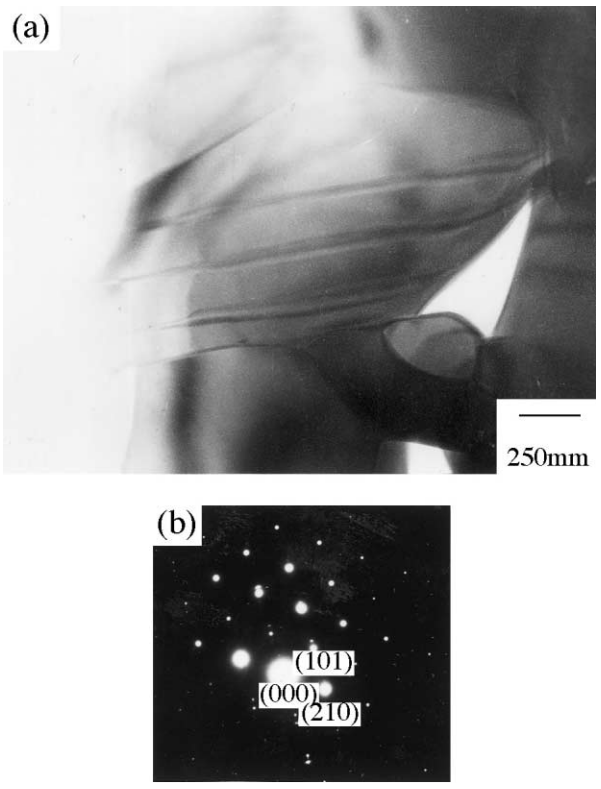

Fig. 9. A $BaTi_4O_9$ grain revealing twinning (a), identified by the selected area diffraction pattern (zone axis: [1 $\bar{2}$ $\bar{1}$]) (b).

suggestion about high interface energy of $Ba_2Ti_9O_{20}$ is misleading. Yu et al.[13] proposed that stress might arise along the crystal structured layers because of the structural factor, which in turn would result in a high potential-energy barrier for nucleation in the reaction. They argued that because the liquid phase arising from adding Bi_2O_3 did not promote the formation rate of $Ba_2Ti_9O_{20}$, the diffusion over a long distance is not a factor for the difficulty in preparing $Ba_2Ti_9O_{20}$. However, as discussed above, diffusion over a long distance is due to the mixing problem, so even the liquid could provide a quick path for ions, it can not improve the mixing. Especially, when liquids occur locally, it would lead to inhomogeneous formation. Moreover, they thought that Al_2O_3 could form $BaAl_2Ti_6O_{16}$, which would intergrow with $Ba_2Ti_9O_{20}$, and thus, decrease the height of the potential-energy barrier. However, this thinking is not convincing because intergrowth is commonly observed in layer-structured ceramics, e.g. in ferrite systems.[24]

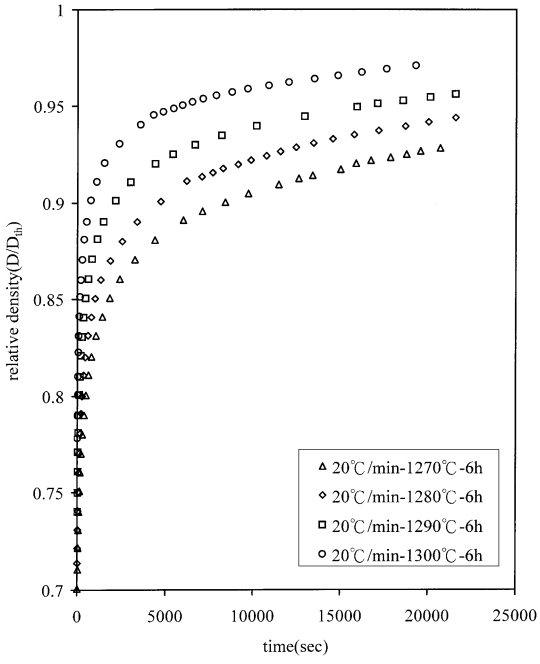

Fig. 10. Relative density versus time at different temperatures for $Ba_2Ti_9O_{20}$.

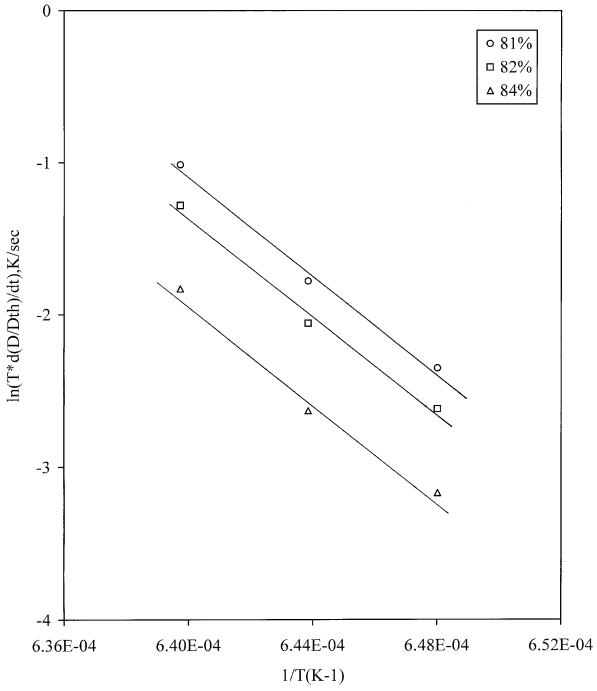

Fig. 11. Evaluation of the activation energy of isothermal sintering of $Ba_2Ti_9O_{20}$.

In Figs. 3 and 4, there are two things that should be pointed out, i.e. when temperatures were $<1200°C$, $BaTi_4O_9$ was still retained but TiO_2 has disappeared and when temperatures were $\geqslant 1200°C$, $Ba_2Ti_9O_{20}$ apparently started to develop. This implies that the Ti species might diffuse in $BaTi_4O_9$ but did not react with $BaTi_4O_9$ to form $Ba_2Ti_9O_{20}$ when temperatures were $<1200°C$, which is supported by the SADP identified as the structure of $BaTi_4O_9$ shown in Fig. 5. Moreover, as observed in SADP, there are extra spots in the diffraction pattern, which implies that the Ti species might diffuse in $BaTi_4O_9$ without reaction and some spots were not spherical indicating that the lattice of $BaTi_4O_9$ was distorted. In Fig. 6, possible $Ba_2Ti_9O_{20}$ nuclei were observed at some local areas of the sample prepared by

the mixture of $BaTi_4O_9$ and TiO_2 calcined at 1200°C for 3 h. Furthermore, the model of nucleation and growth was employed to evaluate the kinetics of solid-state reaction at 1200°C. It was found to have the best fit compared with other models,[17,25,26] shown in Fig. 7. Based on the above discussion, the formation mechanism of $Ba_2Ti_9O_{20}$ could be attributed to the nucleation and growth, and 1200°C should be its nucleation temperature. However, the mechanism for forming the nuclei of $Ba_2Ti_9O_{20}$ is not realized and beyond the scope of this investigation.

The reason why it takes more than 20 more hours to eliminate the tracer amount of $BaTi_4O_9$ should be another issue. When $Ba_2Ti_9O_{20}$was apparently developed (Fig. 4), it was shown in Fig. 9 that most residual $BaTi_4O_9$ grains were found to contain twins, which implies that the remaining grains of $BaTi_4O_9$ were stressed by the surrounding $Ba_2Ti_9O_{20}$ grains. It is evaluated that when $Ba_2Ti_9O_{20}$ nucleated from the matrix of $BaTi_4O_9$ inserted by the Ti species, the structural volume expanded by about 7%, which in turn would stress $BaTi_4O_9$. It should be noted that this evaluation of structural volume change is different from that of Wu and Wang,[8] in which they considered the structural volume change to be due to a direct reaction of $BaTi_4O_9$ and TiO_2 at the interface. Because the remaining $BaTi_4O_9$ was stressed, it would be more difficult for it to nucleate $Ba_2Ti_9O_{20}$, which explains why the residual amount of $BaTi_4O_9$ needs to take a longer time to be eliminated. Inferring from the above discussion, it is considered that to release the stress of the remaining $BaTi_4O_9$ might be a possible way to improve the preparation of $Ba_2Ti_9O_{20}$. Thus, we reground the mixture of $BaTi_4O_9$ and TiO_2 calcined at 1200°C for 3 h and reheated at 1200°C. It was found that $Ba_2Ti_9O_{20}$ could be completely formed in 3 h, which implies that the stressed $BaTi_4O_9$ was released when the sample was reground. The obtained single-phase $Ba_2Ti_9O_{20}$ powder was pressed and sintered at 1390°C without holding. The density, about 99% theoretical density and the grain size about 2–3μm could be achieved, shown in Fig. 12 and the dielectric properties are dielectric constant 39, Q 5863 at 7.3 GHz, and the temperature coefficient of resonance frequency 5 ppm/°C.

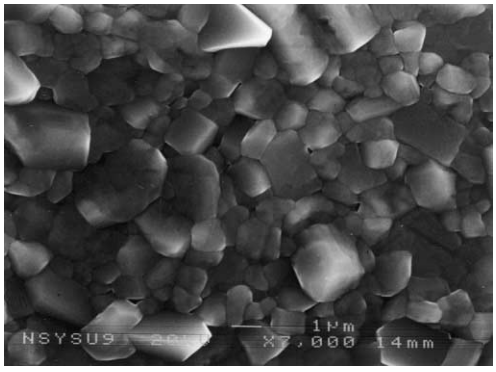

Fig. 12. A uniform microstructure of $Ba_2Ti_9O_{20}$ sintered at 1390°C without holding time with density about 99% theoretical density and grain size 2–3 μm.

5. Conclusions

(1) In preparing $Ba_2Ti_9O_{20}$ by solid-state reaction, the use of the mixture of $BaTi_4O_9$ and TiO_2 is better than that of $BaCO_3$ and TiO_2.

(2) The formation mechanism of $Ba_2Ti_9O_{20}$ might be via the nucleation and growth. It nucleated from the matrix of $BaTi_4O_9$ inserted by the Ti species rather than the direct reaction of $BaTi_4O_9$ and TiO_2 at the interface.

(3) The difficulty in completely forming $Ba_2Ti_9O_{20}$ in a short time might be due to the fact that the remaining $BaTi_4O_9$ grains were stressed by the surrounding $Ba_2Ti_9O_{20}$ grains.

(4) The evaluated activation energy of the isothermal sintering of $Ba_2Ti_9O_{20}$ is about 1320 kJ/mol. High-quality $Ba_2Ti_9O_{20}$ ceramic with a density about 99% theoretical density and the grain size about 2–3 μm could be achieved and the dielectric properties are dielectric constant 39, Q 5863 at 7.3 GHz, and the temperature coefficient of resonance frequency 5 ppm/°C.

Acknowledgements

Supported by the National Science Council under Contract No. NSC 89-2216-E-006-031.

References

1. O'Bryan, H. M., Thomson, J. and Plourde, J. K., A new BaO–TiO_2 compound with temperature-stable high permittivity and low microwave loss. *J. Am. Ceram. Soc.*, 1974, **57**(10), 450–453.
2. Plourde, J. K., Linn, D. F., O'Bryan, H. M. and Thomson, J., $Ba_2Ti_9O_{20}$ as a microwave dielectric resonator. *J. Am. Ceram. Soc.*, 1975, **58**(9-10), 418–420.
3. Plourde, J. K. and Ren, C., Application of dielectric resonators in microwave components. *IEEE Trans. Microwave Theory Tech.*, 1981, **MTT-29**, 754–770.
4. Jonker, G. H. and Kwestroo, W., The ternary system Bao–TiO_2–SnO_2 and BaO–TiO_2–ZrO_2. *J. Am. Ceram. Soc.*, 1958, **41**(10), 390–394.
5. Negas, T., Roth, R. S., Parker, H. S. and Minor, D., Subsolid phase relations in the $BaTiO_3$–TiO_2 system. *J. Solid State Chem.*, 1974, **9**, 297–307.
6. Ritter, J. J., Roth, R. S. and Blendell, J. E., Alkoxide precursor synthesis and characterization of phase in the barium–titanium oxide system. *J. Am. Ceram. Soc.*, 1986, **69**(2), 155–162.
7. Pfaff, G., Peroxide route to synthesize $Ba_2Ti_9O_{20}$. *J. Mater. Sci. Lett.*, 1993, **12**, 32–34.
8. Wu, J. M. and Wang, H. W., Factors affecting the formation of $Ba_2Ti_9O_{20}$. *J. Am. Ceram. Soc.*, 1988, **71**(10), 869–875.
9. Lu, H. C., Burkhart, L. E. and Schrader, G. L., Sol-gel process for the preparation of $Ba_2Ti_9O_{20}$ and $BaTi_5O_{11}$. *J. Am. Ceram. Soc.*, 1991, **74**(5), 968–972.

10. Lin, W. Y. and Speyer, R. F., Fabrication of undoped near-monophase $Ba_2Ti_9O_{20}$ via rapid thermal processing. *J. Mater. Res.*, 1999, **14**(5), 1939–1943.
11. O'Bryan, H. M. and Thomson, J., Phase equilibria in the TiO_2-rich region of the system BaO–TiO_2. *J. Am. Ceram. Soc.*, 1974, **57**(12), 522–526.
12. Jaakola, T., Uusimaki, A. and Leppavuori, S., Importance of homogeneous composition in sintering behavior of $Ba_2Ti_9O_{20}$ ceramics. *Int. J. High Technol. Ceram.*, 1980, **2**, 195–206.
13. Yu, J., Zhan, H., Wang, J. and Xia, F., Effect of Al_2O_3 and Bi_2O_3 on the formation mechanism of Sn-doped $Ba_2Ti_9O_{20}$. *J. Am. Ceram. Soc.*, 1994, **77**(4), 1052–1056.
14. Cullity, B.D., Internal standard method. In *Elements of X-Ray Diffraction*, 2nd edn. Addison-Wesley, New York, 1977, pp. 415–417.
15. Hakki, B. W. and Coleman, P. D., A dielectric resonator method of measuring inductive capacitance in millimeter range. *IEEE Trans. Microwave Theory Tech.*, 1960, **MTT-8**, 402–410.
16. Kobayashi, Y. and Katoh, M., Microwave measurement of dielectric properties of low-loss materials by the dielectric rod resonator method. *IEEE Trans. Microwave Theory Tech.*, 1985, **MTT-33**(7), 586–592.
17. Hulbert, S. F., Models for solid-state reactions in powdered compacts: a review. *J. Br. Ceram. Soc.*, 1969, **6**(1), 11–20.
18. Johnson, W. A. and Mehl, R. F., Reaction kinetics in processes of nucleation and growth. *Trans. AIME*, 1939, **135**, 416–433.
19. Avrami, M., Kinetic of phase change : I. *J. Chem. Phys.*, 1939, **7**(12), 1103–1112; Kinetic of phase change: II, *J. Chem. Phys.*, 1940, **8**(2), 212–224; Kinetic of phase change : III, *J. Chem. Phys.*, 1941, **9**(2), 177–184.
20. Choy, J. H., Han, Y. S., Kim, J. T. and Kim, Y. H., Citrate route to ultra-fine barium polytitanates with microwave dielectric properties. *J. Mater. Chem.*, 1995, **5**(1), 57–63.
21. Javadpour, J. and Eror, N. G., Raman spectroscopy of high titanate phase in the $BaTiO_3$–TiO_2 system. *J. Am. Ceram. Soc.*, 1988, **71**(4), 206–213.
22. Kirby, K. W. and Wechsler, B. A., Phase relations in the barium–titanate–titanium oxide system. *J. Am. Ceram. Soc.*, 1991, **74**(8), 1841–1847.
23. Fang, T.-T., Hwang, J. B.Structural instability and microstructural change of La^{3+}-doped M-type calcium ferrite. *J. Am. Ceram. Soc.*, 1992, **75**(4), 915–919.
24. Alario-Franco, M. A., Vallet-Regi, M., Henche, M. J. R., Gonzalez-Calbet, J. M., grenier, J. C. and Hagenmuller, P., Non-stoichiometry in perovskitelike ferrite. In *Advances in Ceramics*, Vol. 15, ed. F. F. Y. Wang. The American Ceramic Society, Columbus, OH.
25. Jander, W., Reaction in solid state at high temperature. *Z. Anorg. Allg. Chem.* (in German), 1927, **163**, 1–30.
26. Ginstling, A. M. and Brounshtein, B. I., Concerning the diffusion kinetics of reactions in spherical particles. *J. Appl. Chem. USSR*, 1950, **23**, 1327–1338.